Macromol. Symp. **2007**, 259, 337–347

DOI: 10.1002/masy.200751338

Ab Initio Calculation of the Propagation Kinetics in Free Radical Polymerization: Chain Length and Penultimate Effects

Davide Moscatelli, Marco Dossi, Carlo Cavallotti, Giuseppe Storti*

Summary: In this work, Quantum Chemistry is applied to investigate the propagation kinetics in free radical polymerization. Energies, structures and transition state geometries are determined using density functional theory, which combines good accuracy with reasonable computational demand. In particular, B3LYP functional is used to evaluate the exchange and correlation energy with the 6-311+G(d,p) basis sets. The capabilities of the approach with respect to the prediction of the kinetic constants of elementary processes relevant to polymeric systems (propagation reactions) is first tested using literature experimental data as reference values.[1] Namely, two different monomers of industrial relevance have been selected, acrylonitrile and styrene. For such systems, the effect of chain-length on the propagation rate coefficient is examined. Finally, for the selected monomer pair, the relative reactivity (so-called reactivity ratios) is also analyzed, in particular considering the penultimate effect.

Keywords: kinetic; modeling; polymerization; quantum chemistry

Introduction

The propagation reaction is one of the fundamental kinetic events determining the molecular weight of any polymeric material. With reference to free radical polymerization, different experimental techniques (such as pulsed laser polymerization followed by size exclusion chromatography) have been developed to obtain reliable and accurate information about the kinetics of these reactions. However, the experimental determination of rate coefficients is often time consuming or even complicated to achieve because it is hard to study separately the various possible reactions. An alternative could be represented by theoretical predictions based on quantum mechanics, provided that the corresponding computational effort can be managed. In fact, these kinds of reactions are usually difficult to analyze theoretically due to both the large number of atoms present and the different possible chemical pathways involved. On the other hand the rapid and continuing increase in computer power has turned possible to use ab initio quantum mechanics to determine with sufficient accuracy different properties such as molecular geometries (i.e. bond lengths, bond angles and torsional angles), energetic profile of reactions, vibrational frequencies of molecular species, transition state structures and reaction frequency factors. In particular ab initio calculations permits to obtain these useful properties explicitly and directly.[1–4]

The aim of this work is to provide an as rigorous as possible first principle estimation of the propagation kinetic constants in polymeric systems of industrial relevance (acrylonitrile and styrene) adopting quantum chemistry. To test the capabilities of the selected computational approach some relevant parameters (i.e. activation energy and exothermicity) have been determined

---

CFAlab, Politecnico di Milano, via Mancinelli 7, 20131 Milano, Italy
Fax +39-02-2399-3180;
E-mail: davide.moscatelli@polimi.it

and compared with those reported by Fischer and Radom[1] for the same reactive steps. Then, the chain length effect on the propagation rate coefficient has been analyzed with reference to acrylonitrile monomer. The results are qualitatively in agreement with literature experimental evidences, even though the estimated values of the kinetic constants are systematically smaller than the experimental ones of about one order of magnitude. To better understand the reason for this discrepancy and to test if it is due to the presence of a different molecular fragment (coming from the initiator) at the beginning of the polymer chain, the effect of different initiators on the first propagation step has been studied. Finally, the reactivity ratios for the acrylonitrile-styrene system have been evaluated considering explicitly the penultimate effect.

Computational Details

The polymerization reactions investigated in this work are relatively simple molecular processes involving the formation of new carbon-carbon σ bonds at the expense of existing π bonds. Even if these reactions are apparently simple, it is not easy to determine their kinetic constant with reliability because of the lack of experimental data, mainly due to the difficulty of their experimentally determination.[5] In this work all the kinetic constants have been computationally determined adopting quantum chemistry calculations.

The selected quantum chemistry approach was the density functional theory (DFT), which combines a good accuracy with a limited computational demand. The Becke 3 parameters and Lee-Yang-Parr functionals were adopted to evaluate the exchange and correlation energies.[6–7] Such computational approach is the same described in our previous publications involving similar reactions.[8–10] The all electron 6-311 with added polarization and diffusion functions (6-311+G(d,p)) basis set was used in the calculations.[11] Moreover simulations with the 6-31G(d,p) basis set has been made in order to compare our results with those reported by Fisher and Radom.[1] To reduce the computational time necessary for the optimization of the molecular structures, geometries and energies at the PM3 semi-empirical level have been determined first,[12] while the same geometries were used as guesses for new geometry optimizations performed at the higher Quantum Mechanic (QM) level of theory. As a general rule, all geometries were fully optimized with the Berny algorithm. The geometry of each molecular structure was considered stable only after calculating vibrational frequencies and force constants and if no imaginary vibrational frequency was found. Transition state structures were located adopting the synchronous transit-guided quasi Newton method[13] and were characterized by a single imaginary vibrational frequency. All calculations were performed with the Gaussian 03 suite of programs,[14] while all pictures were drawn using Molden 4.2.[15]

Results and Discussion

As anticipated, the capabilities of the computational approach have been tested with respect to the evaluation of activation energy and energetic profile of some relevant reactions involving an unsaturated monomer (acrylonitrile, AN or styrene, St) and different radicals. This step has required to identify a set of reactions whose parameters have been measured with accuracy. Such reactions have been found in [1] where both experimental and computational data are available. In particular, we focused our attention on reactions between acrylonitrile or styrene and four different radicals reported in the literature: $CH_3\cdot$ (methyl radical), Bn (benzyl radical), PEst (2-tert-butoxycarbonyl-2-propyl radical or iso-butyryl radical), and PCN (2-cyano-2-propyl radical). For these radicals, optimized structures are reported in Figure 1 while reaction transition state structures and reaction energetic para-

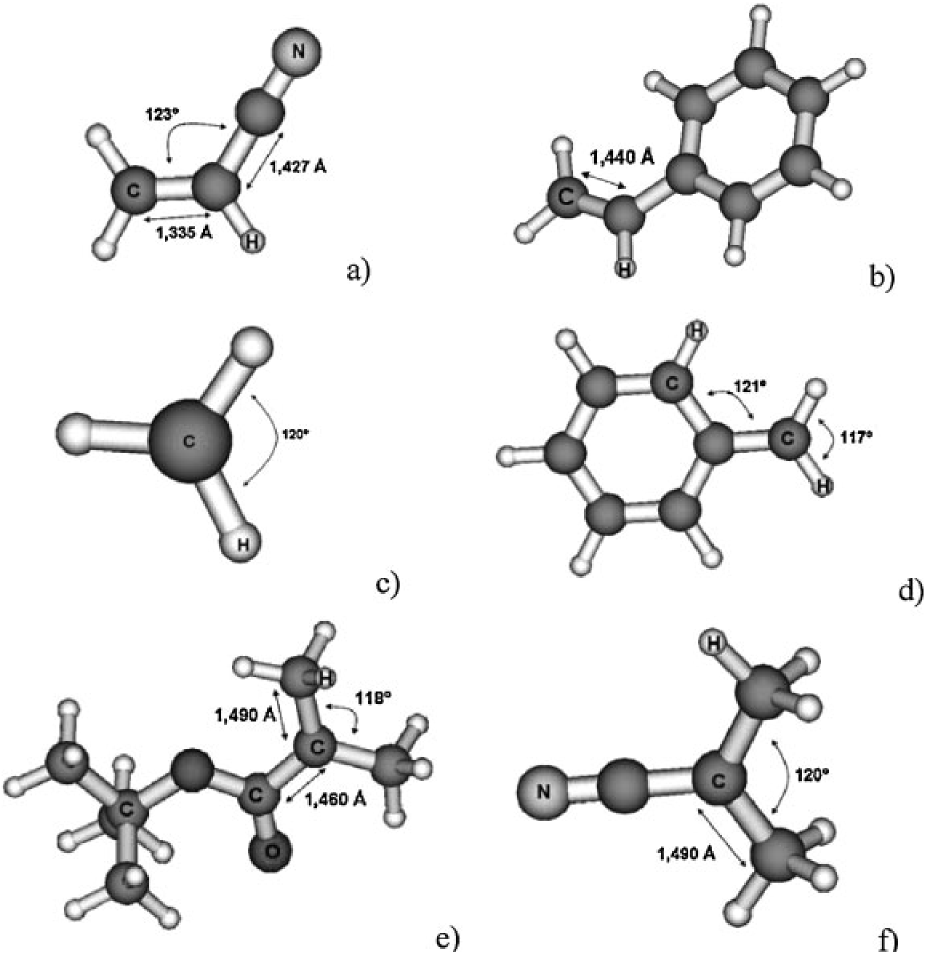

Figure 1.
Optimized molecular structure of monomers and radicals adopted in the simulations: a) acrylonitrile monomer b) styrene monomer, c) $CH_3\cdot$, d) Bn, e) PEst, f) PCN. Geometries are determined at the B3LYP/6-311+G(d,p) level of theory.

meters (enthalpy change and energetic barrier) are shown in Figure 2 and Table 1, respectively.

The numerical values reported in Table 1 are in agreement with those reported by Fischer and Radom. In particular, B3LYP/6-31G(d,p) calculations provide a good estimation of the energetic barriers (deviation from experimental data is less than 10 kJ/mol in each case). About B3LYP/6-311+G(d,p), the results in terms of activation energy are very accurate in some cases, with a deviation from the experimental data less than 2 kJ/mol. On the other hand the deviations from experiment increase with increasing basis-set size for other reactions, thus meaning that the good agreement observed for B3LYP/6-31G(d,p) is partially fortuitous. In terms of enthalpy changes, we observed that B3LYP/6-31G(d,p) systematically overestimates exothermicity while the larger basis set underestimate these energetic data. Finally, these results are in agreement with those reported in ref.[1] Despite the reported deviations from experiments, the Becke 3 parameters and Lee-Yang-Parr functionals permits to obtain good results

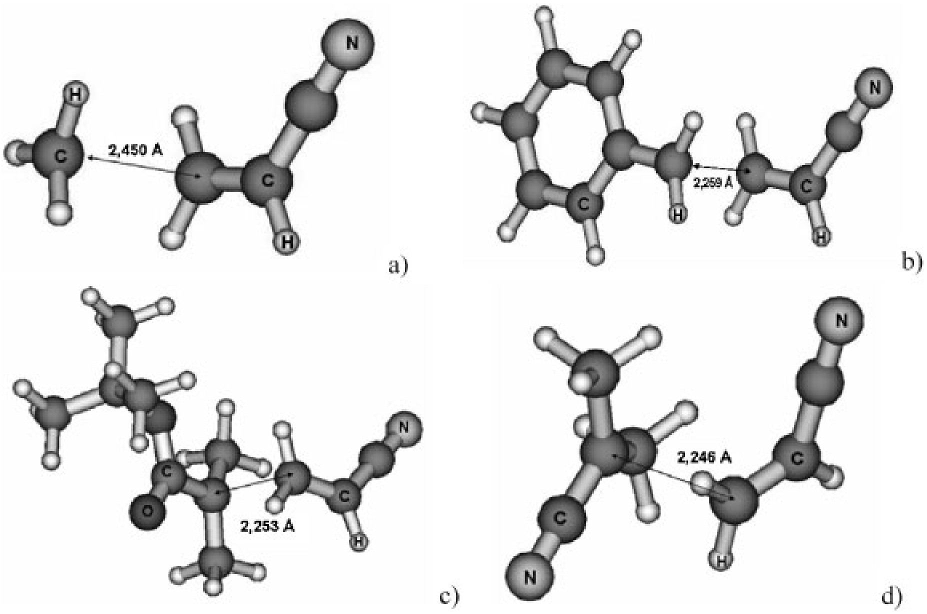

Figure 2.
Optimized transition state structure of reactions between acrylonitrile and radicals reported in [1]: a) $CH_3\cdot$, b) Bn, c) PEst, d) PCN. Geometries are determined at the B3LYP/6-311+G(d,p) level of theory.

with accuracy which is usually below the experimental error, thus indicating this computational approach as an effective semi-quantitative tool to predict kinetics in polymeric systems.

Chain Length Effect

The advent of powerful analytic techniques in the last decades, in particular the pulsed laser polymerization (PLP) followed by size-exclusion chromatography (SEC), allowed the accurate determination of the individual propagation rate coefficient k_p.[16] While k_p is frequently considered independent of the radical chain length, recent results have shown that the propagation constant is a function of degree of polymerization.[17–20] This dependence is restricted to the first propagation steps, until the chain length reaches value of three or four monomer units; in addition Olaj and co-workers quantify the ratio between these propagation rates and the value of k_p^∞ (i.e. the one independent upon the

Table 1.
Comparison between activation energy and reaction enthalpy, both theoretically and experimentally determined, for different AN-radical and St-radical reactions. Energies are reported in kJ/mol.

Reaction	B3LYP/6-31G(d,p)		B3LYP/6-311+G(d,p)		Experimental[1]	
	ΔH	E_a	ΔH	E_a	ΔH	E_a
AN + $CH_3\cdot$	−139.5	7.6	−123.5	13.8	−125.0	15.4
AN + Bn	−73.1	22.6	−59.0	29.9	–	29.1
AN + PEst	−59.9	24.6	−46.4	31.7	–	23.3
AN + PCN	−55.8	33.9	−38.5	39.3	–	24.8
St + $CH_3\cdot$	−148.3	11.1	−124.7	17.2	−144.0	17.5
St + Bn	−69.3	27.1	−54.6	35.1	–	30.8
St + PEst	−59.2	26.1	−45.8	34.7	–	21.5
St + PCN	−56.7	31.0	−45.5	37.4	–	24.3

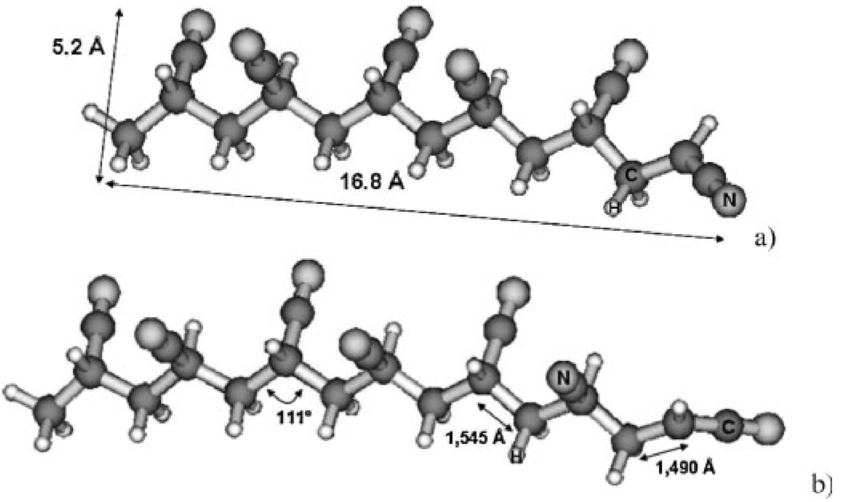

Figure 3.
Optimized structures of acrylonitrile chains composed by 6 (a) and 7 (b) monomers in a syndiotactic conformation.

chain length) and they found that k_p changes of about 25–30% in these first reactive steps.[16,19] From the chemical point of view, such dependence upon the chain length is expected and this experimental evidence should be used to build a more reliable description of free radical polymerization kinetics.[19,21] Adopting the computational approach previously described, it has been determined the chain length effect in the polymerization of acrylonitrile. The growing AN chain has been modeled with a syndiotactic oligomer composed by up to 7 monomers (optimized geometries of hexamer and heptamer are shown in Figure 3).

Kinetic constants of the first propagation steps are determined adopting both 6-31G(d,p) and 6-311+G(d,p) basis set. The calculated rate coefficients are shown in Table 2 and the transition state of reaction that produces heptamer-radical is shown in Figure 4.

The results reported in Table 2 indicate the same behaviour in the determination of enthalpy changes and activation energies as previously reported whatever the selected basis set. By close inspection of the predicted values, the chain length effect in the propagation rate becomes apparent, even though, comparing these results with those reported in literature, the estimated values of the kinetic constants are systematically smaller than the experimental ones of about one order of magnitude.[22] In particular, adopting the smaller basis set,

Table 2.
Calculated values of the enthalpy changes, activation energies and rate constants for the first propagation reactions. Energies are reported in kJ/mol while k_p in cm^3/mol/s and expressed as: $k_p = A \cdot T \cdot \exp(-E_a/RT)$.

Reaction	B3LYP/6-31G(d,p)			B3LYP/6-311+G(d,p)		
	ΔH	E_a	k_p @ 300 K	ΔH	E_a	k_p @ 300 K
$AN + I\cdot \rightarrow R_1\cdot$	−71.8	29.0	2.76E+06	−59.8	35.0	8.11E+05
$AN + R_1\cdot \rightarrow R_2\cdot$	−71.9	31.4	1.88E+06	−59.6	37.8	8.70E+04
$AN + R_2\cdot \rightarrow R_3\cdot$	−69.9	33.1	9.28E+05	−57.4	39.7	6.03E+04
$AN + R_3\cdot \rightarrow R_4\cdot$	−70.0	33.4	8.52E+05	–	–	–
$AN + R_4\cdot \rightarrow R_5\cdot$	−69.5	33.6	7.11E+05	–	–	–
$AN + R_6\cdot \rightarrow R_7\cdot$	–	–	–	−56.9	40.4	4.86E+04

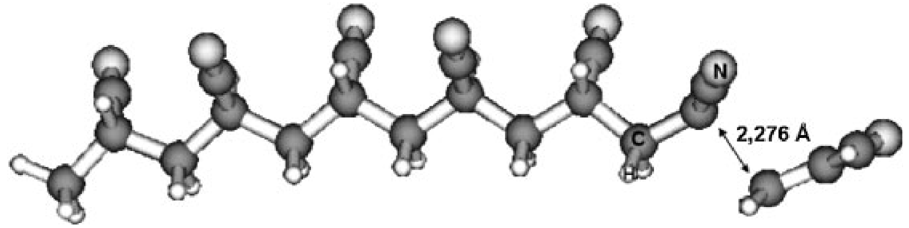

Figure 4.
Optimized transition state structure of propagation reaction that brings to an acrylonitrile chain composed by 7 monomers.

the propagation rate for the first five steps has been determined and the ratio between k_p^7 and k_p^1 was found equal to 0.258. Furthermore, the ratio between two consecutive propagation steps becomes smaller at increasing chain length, passing from 0.68 (k_p^2/k_p^1) to 0.84 (k_p^7/k_p^6): such result confirms that the chain length effect is limited to the first few propagation steps. Comparable evidences have been found adopting the larger basis set that has been used to determine the propagation rate until the heptamer-radical production. Also with this basis set it was possible to describe the chain length effect qualitatively only, since the determined rate coefficients are smaller than the experimental ones.

To better understand this finding, the effect of initiator on these first propagation steps has been explicitly analyzed. As a matter of fact, the PCN radical (a methyl group substituted by a hydrogen, $CH_3CNCH\cdot$) has been used in all previous simulations. However, different initiators are mostly used in literature experiments and a dependence on the propagation rate on the type of initiating fragment can be reasonably expected. Such an effect should be more significant for small molecules, i.e. the shorter is the chain length of the growing radical.

Initiator Effect

To test the possibility that the initiator plays an important role in the first propagation steps, the propagation rate for the first three reaction steps has been evaluated starting from AN and three widely used initiators: azobis-isobutyronitrile (AIBN) that decomposes into two 2-cyanoprop-2-yl radicals eliminating a nitrogen molecule; di-t-butyl peroxide (DTBP) that produces two terbutyloxy radicals and dibenzoyl peroxide (DBP) that decomposes into carbon dioxide and phenyl radicals. In Figure 5, the optimized geometry of these initiators is shown together with the active radical that they produce, while in Figure 6 we reported the computed structure of some products of the reactions involving different initiators.

The estimated values of the kinetic constants corresponding to the different commercial initiators are summarized in Table 3. For each kinetic step, we reported: enthalpy change, activation energy, pre-exponential factor and k_p value determined at 300 K. Focusing first on the enthalpy changes, the presence of a different initiator fragment drastically influences the value. This is particularly evident in the case of the phenyl radical (that is the most reactive between those selected in this work) where the estimated enthalpy change passes from −166.5 kJ/mol for reaction 7 to about −60.0 kJ/mol for both reactions 8 and 9. For the reaction between AN and 2-cyanoprop-2-yl radical, the enthalpy change differs of about 20 kJ/mol with respect to successive reactive steps, while the difference is about 27 kJ/mol for the terbutyloxy radical. The predicted data show how the kinetic constants are less affected by the presence of AIBN than by the other two initiators. This is due to the particular molecular geometry of the 2-cyanoprop-2-yl radical, which is very similar to those adopted for the reactions reported in the chain length effect section. For the other two systems,

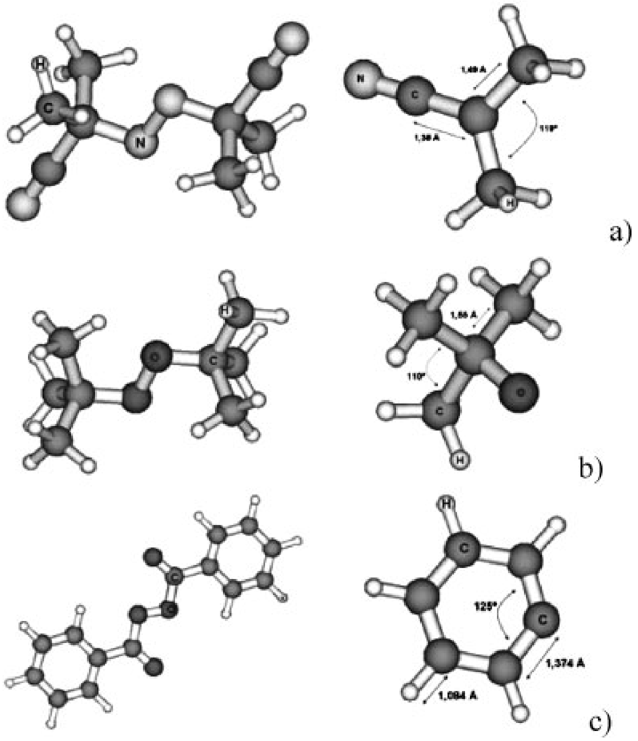

Figure 5.
Optimized molecular structure of initiator adopted in the simulations and geometries of relative radicals produced: a) AIBN, b) t-butyl peroxide, c) dibenzoyl peroxide.

the first reaction is widely affected by the presence of both terbutyloxy and phenyl radicals (the transition state structures of the reactions between AN and both phenyl and 2-cyanoprop-2-yl radical are shown in Figure 7). Notably, the calculated ratios between the rate coefficients corresponding to subsequent kinetic steps following the first one, i.e. the one involving monomer and initiator, are not far from 1. Thus, we can conclude that the initiator effect is not comparable with the chain length effect, at least for the specific system under examination (AN monomer).

Finally, a few comments about possible improvements of the predictions of first propagation constants and chain length effect. First of all, more accurate predictions of the pre-exponential factors should be achieved. As reported in our previous work,[8] while computed results for polymeric systems are more accurate in terms of activation energy, the explicit consideration that lower vibrational frequencies can be attributed to torsion around sp^3 bonds of the main polymer chain leads to a more reliable description of the vibrational and rotational partition function and then to improved estimation of the pre-exponential factors.[8] Secondly, the chain length effect must be due to steric effects (considered in the pre-exponential factor) more than energetic ones (reflected in the activation energy). Accordingly, next efforts in the computational estimation of chain length effect will be focused on the determination of partition functions associated to such torsion in the harmonic approximation.

Penultimate Effect

With reference to free-radical copolymerization, the classical terminal model proposed by Lewis and Mayo has been clearly demonstrated to be incapable to simulta-

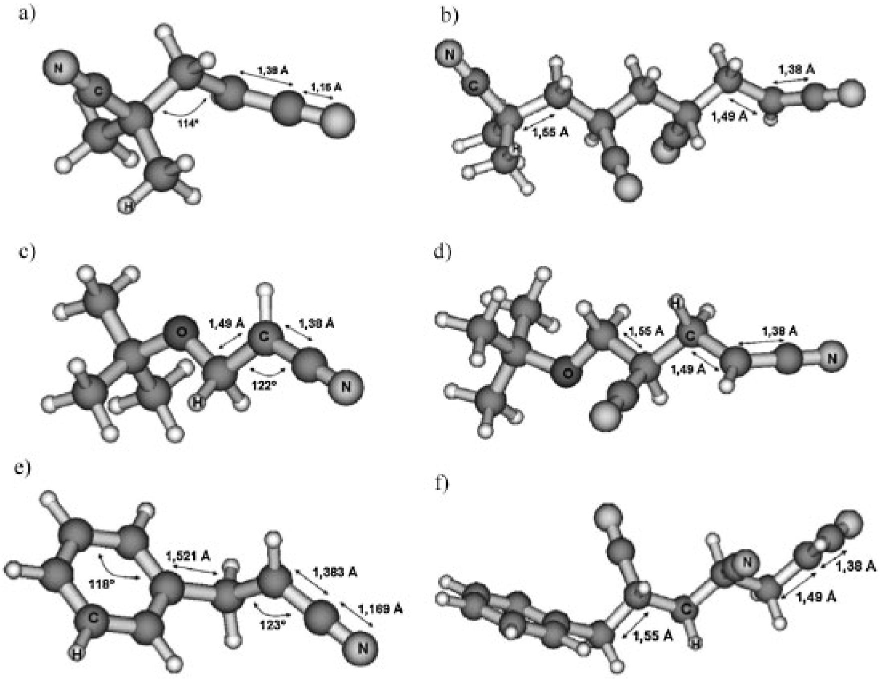

Figure 6.
Optimized molecular structure of oligomers produced as a result of reactions named in Table 3: a) 1, b) 3, c) 4, d) 5, e) 7, f) 9. Geometries are determined at the B3LYP/6-311+G(d,p) level of theory.

neously describe overall propagation rate and evolution of the copolymer composition in many polymeric systems. The so-called penultimate effect has been proposed to better describe propagation kinetics in copolymerization. In particular, an explicit penultimate unit effect occurs when the propagation rate is affected by both the terminal and the penultimate units of the growing radical and also it is dependent by the type of monomer that reacts with the propagating chain. Experimental evidences suggested that the explicit penultimate model should be considered in the majority of copolymerization reactions.[23–25]

Taking advantage of the estimated rate coefficients for the homo-polymerization of

Table 3.
Calculated values of the enthalpy changes, activation energies, pre-exponential factors and rate constants for the first propagation reactions. Energies are reported in kJ/mol while k_p in $cm^3/mol/s$ and expressed as: $k_p = A \cdot T \cdot \exp(-E_a/RT)$.

#	Reaction	B3LYP/6-311+G(d,p)			
		ΔH	E_a	$Log_{10}A$	k_p @ 300 K
1	$AN + AIBN^{radical} \rightarrow R\cdot_1^{AIBN}$	−38.5	39.4	11.566	5.19E+04
2	$AN + R\cdot_1^{AIBN} \rightarrow R\cdot_2^{AIBN}$	−59.6	39.1	11.406	3.99E+04
3	$AN + R\cdot_2^{AIBN} \rightarrow R\cdot_3^{AIBN}$	−59.9	37.5	11.527	1.01E+05
4	$AN + t\text{-}but\text{-}O\cdot \rightarrow R\cdot_1^{t-butO}$	−87.5	19.7	11.442	1.03E+08
5	$AN + R\cdot_1^{t\text{-}butO} \rightarrow R\cdot_2^{t\text{-}butO}$	−62.7	39.5	11.736	7.25E+04
6	$AN + R\cdot_2^{t\text{-}butO} \rightarrow R\cdot_3^{t\text{-}butO}$	−59.1	38.6	11.562	6.93E+04
7	$AN + Ph\cdot \rightarrow R\cdot_1^{Ph}$	−166.5	2.7	12.589	1.33E+12
8	$AN + R\cdot_1^{Ph} \rightarrow R\cdot_2^{Ph}$	−59.8	34.9	11.258	1.52E+05
9	$AN + R\cdot_2^{Ph} \rightarrow R\cdot_3^{Ph}$	−59.2	37.9	11.667	1.18E+05

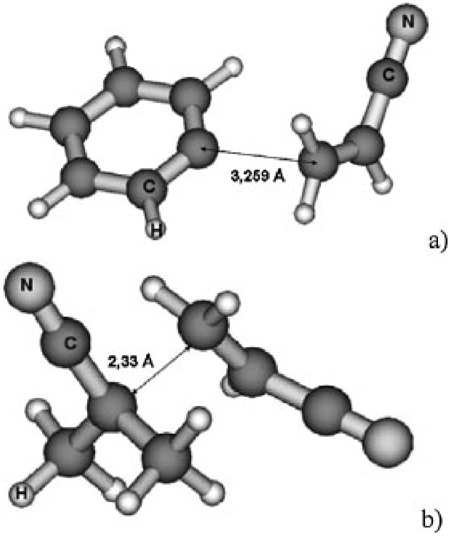

Figure 7.
Optimized transition state structure of reaction between acrylonitrile monomer and radical produced from: a) dibenzoyl peroxide and b) AIBN. Geometries are determined at the B3LYP/6-311+G(d,p) level of theory.

styrene reported in a previous paper,[8] in this work the propagation rates in the copolymer styrene-acrylonitrile are estimated taking into account the explicit penultimate unit effect. In particular, the corresponding two reactivity ratios have been evaluated adopting the same computational method reported above and compared with available experimental data. Namely, to minimize the computational effort, the growing chain has been described as a trimer. The results of these simulations are summarized in Table 4 while the transition state structures of each reaction are sketched in Figure 8.

Using the kinetic constants in Table 4, the corresponding reactivity ratios have been estimated from the following definitions:

$$r_{11} = \frac{r^{1}_{AN-AN-AN}}{r^{2}_{AN-AN-St}}$$

$$r_{21} = \frac{r^{3}_{St-AN-AN}}{r^{4}_{St-AN-St}}$$

The values calculated this way are $r_{11} = 0.011$ and $r_{21} = 0.384$, respectively, to be compared with the corresponding literature values of 0.259 and 0.514. Such estimation is definitely quite rough, since longer polymeric chains should be accounted for to improve the reliability of the predicted values; in fact, by assuming the reacting chain as made of three monomer units only, the predicted values of the kinetic constants of homo-polymerization at 300 K were 2.66 10^5 and 1.88 10^6 cm^3/mol/s for styrene and acrylonitrile, respectively. However, considering the growing chain formed by five monomer units, the same propagation rate coefficients were predicted as 1.98 10^5 and 8.52 10^5 cm^3/mol/s, thus indicating that three monomer units are not enough to achieve predictions corresponding to long chains. Such expectation has been confirmed also for copolymers, where the ratio of the estimated rate coefficients for trimer and pentamer resulted equal to 0.74 for styrene and 2.20 for acrylonitrile, respectively. To conclude, these results should be regarded as a first approximation and longer radicals will be considered to achieve reliable predictions.

Table 4.
Calculated values of the enthalpy changes, activation energies, pre-exponential factors and rate constants for the propagation reactions involved in the determination of r_{11} and r_{21} reactivity ratio. Energies are reported in kJ/mol while k_p in cm^3/mol/s and expressed as: $k_p = A \cdot T \cdot \exp(-E_a/RT)$.

Reaction		B3LYP/6-311+G(d,p)			
		ΔH	E_a	$Log_{10}A$	k_p @ 300 K
$r^1_{AN-AN-AN}$	AN-AN · + AN → AN-AN-AN·	−59.6	37.8	11.524	8.70E+04
$r^2_{AN-AN-St}$	AN-AN · + St → AN-AN-St·	−68.4	26.9	11.592	8.28E+06
$r^3_{St-AN-AN}$	St-AN · + AN → St-AN-AN·	−60.7	35.1	11.752	4.38E+05
$r^4_{St-AN-St}$	St-AN · + St → St-AN-St·	−65.4	30.9	11.431	1.14E+06

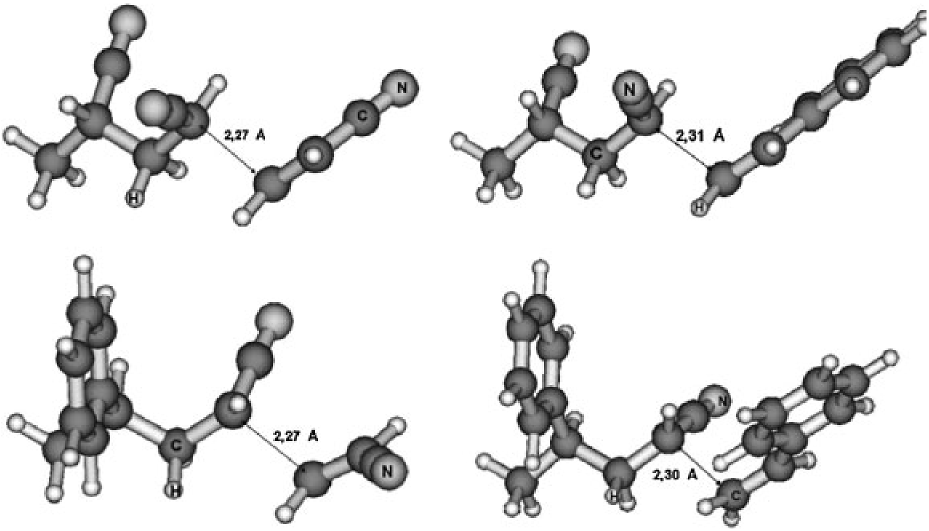

Figure 8.
Optimized transition state structure of reaction named in Table 4: a) $r_{AN\text{-}AN\text{-}AN}$, b) $r_{AN\text{-}AN\text{-}St}$, c) $r_{St\text{-}AN\text{-}AN}$, d) $r_{St\text{-}AN\text{-}St}$. Geometries are determined at the B3LYP/6-311+G(d,p) level of theory.

Conclusions

In this work, propagation kinetics in free radical polymerization have been studied using quantum chemistry. All the kinetic constants have been calculated using density functional theory and adopting classic transition state theory. Both B3LYP/6-31G(d,p) and B3LYP/6-311+G(d,p) give results in good agreement with available experimental data. The effect of the chain length of the reacting radicals has been investigated and the results are qualitatively in agreement with literature experimental evidences. However, more correct descriptions of the vibrational and rotational partition function is needed to improve the quantitative performance of such predictions. Finally, for styrene and acrylonitrile monomer pair, reactivity ratios have been also analyzed considering the explicit penultimate unit effect. The obtained results are affected by the length of the used chain model and longer chains are required to rule out the effect of chain length on the predicted reactivity ratios.

[1] H. Fischer, L. Radom, *Angew. Chem. Int. Ed.* **2001**, *40*, 1340.

[2] J. P. A. Heuts, R. G. Gilbert, L. Radom, *J Phys. Chem.* **1996**, *18*, 997.

[3] R. G. Balderas, M. L. Coote, D. J. Henry, L. Radom, *J. Phys. Chem. A* **2004**, *108*, 2874–2883.

[4] J. S. S. Toh, D. M. Huang, P. A. Lovel, R. G. Gilbert, *Polymer* **2001**, *42*, 1915–1920.

[5] M. C. Grady, W. J. Simonsick, R. A. Hutchinson, *Macromol. Symp.* **2002**, *182*, 149.

[6] A. D. Becke, *J. Chem. Phys.* **1993**, *98*, 5648.

[7] C. Lee, W. Yang, R. G. Parr, *Phys. Rev. B*, **1988**, *37*, 785.

[8] D. Moscatelli, C. Cavallotti, M. Morbidelli, *Macromolecules* **2006**, *39*, 9641–9653.

[9] S. Fascella, C. Cavallotti, R. Rota, S. Carra', *J. Phys. Chem. A* **2004**, *108*, 3829–3843.

[10] S. Fascella, C. Cavallotti, R. Rota, S. Carra', *J. Phys. Chem. A* **2005**, *109*, 7546–7557.

[11] A. D. Becke, *J. Chem. Phys.* **1993**, *98*, 5648–5652.

[12] J. J. P. Stewart, *J. Comput. Chem.* **1989**, 10.

[13] C. Peng, P. Y. Ayala, H. B. Schlegel, M. J. Frisch, *J. Comp. Chem.* **1996**, *17*, 49.

[14] Gaussian 03, Revision C.02, M. J. Frisch, G. W. Trucks, H. B. Schlegel, G. E. Scuseria, M. A. Robb, J. R. Cheeseman, J. A. Montgomery, Jr., T. Vreven, K. N. Kudin, J. C. Burant, J. M. Millam, S. S. Iyengar, J. Tomasi, V. Barone, B. Mennucci, M. Cossi, G. Scalmani, N. Rega, G. A. Petersson, H. Nakatsuji, M. Hada, M. Ehara, K. Toyota, R. Fukuda, J. Hasegawa, M. Ishida, T. Nakajima, Y. Honda, O. Kitao, H. Nakai, M. Klene, X. Li, J. E. Knox, H. P. Hratchian, J. B. Cross, V. Bakken, C. Adamo, J. Jaramillo, R. Gomperts, R. E. Stratmann, O. Yazyev, A. J. Austin, R. Cammi, C. Pomelli, J. W.

Ochterski, P. Y. Ayala, K. Morokuma, G. A. Voth, P. Salvador, J. J. Dannenberg, V. G. Zakrzewski, S. Dapprich, A. D. Daniels, M. C. Strain, O. Farkas, D. K. Malick, A. D. Rabuck, K. Raghavachari, J. B. Foresman, J. V. Ortiz, Q. Cui, A. G. Baboul, S. Clifford, J. Cioslowski, B. B. Stefanov, G. Liu, A. Liashenko, P. Piskorz, I. Komaromi, R. L. Martin, D. J. Fox, T. Keith, M. A. Al-Laham, C. Y. Peng, A. Nanayakkara, M. Challacombe, P. M. W. Gill, B. Johnson, W. Chen, M. W. Wong, C. Gonzalez, J. A. Pople, Gaussian, Inc., Wallingford, CT **2004**.

[15] G. Schaftenaar, J. H. Noordik, *J. Comput. -Aided Mol. Design* **2000**, *14*, 123–134.

[16] S. Beuermann, *Macromolecules* **2002**, *35*, 9300–9305.

[17] O. F. Olaj, I. Bitai, F. Hinkelmann, *Makromol. Chem.* **1987**, *188*, 1689.

[18] O. F. Olaj, I. Schnoell-Bitai, *Eur. Polym. J.* **1989**, *25*, 635.

[19] O. F. Olaj, M. Zoder, P. Vana, A. Kornherr, I. Schnoell-Bitai, G. Zifferer, *Macromolecules* **2005**, *38*, 1944–1948.

[20] G. B. Smith, T. Russell, M. Yin, J. P. A. Heuts, *Eur. Polym. J.* **2005**, *41*, 225–230.

[21] A. N. Nikitin, A. V. Evseev, *Macromol. Theory Simul.* **1999**, *8*, 296–330.

[22] J. P. A. Heuts, G. T. Russell, *Eur. Polym. J.* **2006**, *42*, 3–20.

[23] M. L. Coote, T. P. Davis, *Macromolcules* **1999**, *32*, 3626–3636.

[24] M. L. Coote, T. P. Davis, *Macromolcules* **1999**, *32*, 5270–5276.

[25] M. L. Coote, T. P. Davis, *Prog. Polym. Sci.* **1999**, *24*, 1217–1251.